Investigation of mechanical, material and compositional determinants of human trabecular bone quality in type 2 diabetes

Praveer Sihota[a †], Ram Naresh Yadav[a †], Ruban Dhaliwal[b], Jagadeesh Chandra Bose[c], Vandana Dhiman[d], Deepak Neradi[e], Shailesh Karn[e], Sidhartha Sharma[e], Sameer Aggarwal[e], Vijay G. Goni[e], Vishwajeet Mehandia[a], Deepak Vashishth[f], Sanjay Kumar Bhadada[d*], Navin Kumar[a*]

[a]*Department of Mechanical Engineering, Indian Institute of Technology Ropar, Rupnagar, Punjab, 140001, India*

[b]*Metabolic Bone Disease Center, State University of New York, Upstate Medical University, Syracuse, NY, USA*

[c]*Department of Internal Medicine, Post Graduate Institute of Medical Education and Research, Chandigarh, 160012, India*

[d]*Department of Endocrinology, Post Graduate Institute of Medical Education and Research, Chandigarh, 160012, India*

[e]*Department of Orthopedics, Post Graduate Institute of Medical Education and Research, Chandigarh, 160012, India*

[f]*Department of Biomedical Engineering, Center for Biotechnology and Interdisciplinary Studies, Rensselaer Polytechnic Institute, Troy, NY, USA*

* All correspondence and requests regarding manuscript should be addressed to S.K.B. (Telephone: +91-987-660-2448; email: bhadadask@rediffmail.com) ORCiD: 0000-002-0410-8778 or N.K. (Telephone: +91-950 121-2380; email: nkumar@iitrpr.ac.in) ORCiD: 0000-0002-7958-8155

† Equal Contribution

Disclosure Statement: The authors have nothing to disclose.

Abstract

Context: Increased bone fragility and reduced energy absorption to fracture associated with type 2 diabetes (T2D) cannot be explained by bone mineral density alone. This study, for the first time reports on alterations in bone tissue's material properties obtained from individuals with diabetes and known fragility fracture status.

Objective: To investigate the role of T2D in altering biomechanical, microstructural and compositional properties of bone in individuals with fragility fracture.

Design: Femoral head bone tissue specimens were collected from patients who underwent replacement surgery for fragility hip fracture. Trabecular bone quality parameters were compared in samples of two groups: non-diabetic (n=40) and diabetic (n=30), with a mean duration of disease 7.5±2.8 years.

Results: No significant difference was observed in aBMD between the groups. Bone volume fraction (BV/TV) was lower in the diabetic group due to fewer and thinner trabeculae. The apparent-level toughness and post-yield energy were lower in those with diabetes. Tissue-level (nanoindentation) modulus and hardness were lower in this group. Compositional differences in diabetic group included lower mineral:matrix, wider mineral crystals, and bone collagen modifications - higher total fAGEs, higher non-enzymatic-cross-link-ratio (NE-xLR), and altered secondary structure (Amide bands). There was a strong inverse correlation between NE-xLR and post-yield-strain, fAGEs and post-yield energy, and, fAGEs and toughness.

Conclusion: Current study is novel in examining bone tissue in T2D following first hip fragility fracture. Our findings provide evidence of hyperglycemia's detrimental effects on trabecular bone quality at multiple scales leading to lower energy absorption and toughness-indicative of increased propensity to bone fragility.

Keywords: Diabetes; Bone quality; AGEs; trabecular bone; fragility fracture, bone toughness

INTRODUCTION:

Type 2 diabetes (T2D) affects bone homeostasis leading up to three-fold increased hip fracture risk compared to those without diabetes (1–3). This high fragility fracture risk is observed despite adequate areal bone mineral density (aBMD) in T2D (4–9). Thus, aBMD underestimates fracture risk in T2D, making the clinical identification of those at risk for fractures difficult. Beyond aBMD, the key factors contributing to bone strength are the parameters of bone quality – microstructure, bone material properties, bone mineral content and mean crystal size, bone protein (Amide I and II) quantity and its secondary structure, and the bone cell activity and dynamics **(Figure 1A)**. These determinants have been examined individually in few studies and material properties are often listed as the cause of poor bone quality in diabetes (10–13). Only animal studies (14–19) and three recent studies of human tissue have attempted to address this question comprehensively (10,11,13). A limitation of the previous human studies is that bone tissue was collected at the time of arthroplasty and may therefore have confounding effects associated with arthritis (including increased trabecular bone density) (10,11,13). Furthermore, no prior studies of bone tissue material properties in humans have been conducted with known diabetic status and known fragility fracture status. The current study is novel in examining human bone tissue following first hip fragility fracture.

The mechanisms underlying this poor bone quality and high fracture risk in diabetes are not well understood. Prolonged hyperglycemia leads to an increase in the non-enzymatic reactions (Maillard reactions) and the formation of advanced glycation end-products (AGEs) through post-translation modification (20). AGEs then accumulate in the bone tissue and react irreversibly with amino acid residues of peptides or proteins to form protein adducts or protein crosslinks (21). This phenomenon, widely recognized as non-enzymatic cross-linking (NE-xL), is the underlying mechanism for multiple complications of diabetes, as it alters normal cellular functioning and tissue quality (22,23). AGE accumulation may also alter mineralization through hyperglycemia affecting bone strength (15).

In the present *ex vivo* study, we aimed for multi-scale characterization of bone tissue from individuals with and without diabetes, following hip fracture. This study includes - investigation of the structural parameters at voxel size consistent with use of micro computed tomography (μ-CT) and corresponding apparent level mechanical properties measued through the uniaxial compression test. We also examine bone material properties

(nanoindentation) as well as bone composition [thermogravimetric analysis (TGA)], mineral crystal size [X-ray diffraction (XRD)], alterations in protein content, enzymatic (E-xLR), non-enzymatic cross-link ratio (NE-xLR) [Fourier transform infrared spectroscopy (FTIR)], and fAGE content in the human diabetic bone tissue.

MATERIAL AND METHODS:

Study Participants

Bone samples were taken from two groups of patients who underwent bipolar hemiarthroplasty or total hip replacement following fragility fracture of hip - patients without diabetes (n=40) and with diabetes (n=30). Replacement surgery was the recommended treatment as these hip fractures were unsuitable for management with cannulated cancellous screw or proximal femoral nail. Patients' age also favored replacement surgery for better outcome. Type 2 diabetes mellitus was diagnosed according to the American Diabetes Association criteria (24). None of the patients had history of hip fracture prior to the fracture reported here. Patients with cancer, osteoarthritis, renal dysfunction, primary or secondary hyperparathyroidism, unexplained elevated alkaline phosphatase, and secondary osteoporosis (chronic steroid or antiepileptic use) were excluded from the study.

All patients with diabetes were taking anti-diabetic medications (metformin, sulfonylurea, or insulin). None were on pioglitazone or SGLT2 inhibitors. All participants involved in the study were from Northern India. The study was approved by the Institutional Ethics Committee (Approval Number PGI/IEC/2015/171) of the Postgraduate Institute of Medical Education and Research, Chandigarh. Written informed consent was obtained from each study participant. Demographic, clinical, biochemical and aBMD (contralateral femoral neck BMD) were recorded for all participants.

Sample Procurement and Storage:

Femoral heads were collected from patients undergoing replacement surgery for hip fractures. From each femoral head 5-7 cylindrical trabecular bone cores, each 5 mm in diameter and 8-9 mm in length, were extracted from femoral heads along the direction of the principal trabeculae using the drilling machine attached with diamond core bit as shown in (**Figure 1B)**. The bone cores were cleaned with a water jet, wrapped in saline-soaked gauze (PBS 7.4 pH), transferred into sample bags, labeled, and subsequently stored at -20°C(10).

Bone cores were then used for different characterization techniques, as shown in **(Figure 1C)**. All experiments were conducted within one month after the collection of the femoral head.

Assessment of Bone quality parameters:

Microstructural parameters

The microstructural parameters were studied by using *μ-CT*. One bone core of each patient was air-dried and scanned along the cylindrical axis on a micro-CT system (Phoenix/x-ray, GE Sensing & Inspection Technologies, Germany) using 10 μm voxel size, 45 keV tube voltage, 250 μA beam current, 250 sec integration time and 10 frames. Reconstruction of scanned images was collected using Phoenix software (phoenix/x-ray, GE Measurement & Control; Germany) and reconstructed images were imported in Scan-IP (Simpleware Ltd, UK) and Image J's plugin BoneJ [software by National Institute of Health, available at (https://imagej.nih.gov/ij/)](25). Following structural parameters were obtained: bone volume fraction (BV/TV), trabecular thickness (Tb.Th), trabecular separation (Tb.Sp), trabecular number (Tb.N), structure model index (SMI), and degree of anisotropy (DA) (26).

Bulk mechanical properties

After μ-CT imaging, the bone cores were utilized for compression testing. The samples were rehydrated in saline-soaked gauzes for 2 hours at 4°C. Mean specimen length of 8 mm and length to diameter ratio of nearly 1.5:1 was used for testing. The bone cores were glued in customized mild steel cylindrical end caps to minimize end-effects (27). Compression test was performed on each core to measure the mechanical properties using an electromagnetic testing system (Electroforce 3200, Bose, Eden Prairie, MN, USA with specification of load cell: ±450N, and LVDT: stroke length ±6.5mm with 0.1μm resolution) at room temperature while keeping the specimen hydrated in PBS spray (28). The specimens were preloaded to 5N to ensure proper contact between the test specimen and the compression plate. Then, preconditioning between 0.05 to 0.2 % strain was done in three cycles to minimize the toe region. Montontic testing was conducted at a strain rate of 0.01 s^{-1} until 1 mm displacement. The load-displacement data were captured at 100 Hz frequency and converted into stress-strain data shown in **(Figure 2A)**, to determine several mechanical parameters including elastic modulus, yield point (using the 0.2% offset method), ultimate point (determined as the point of maximum load), post-yield strain (determined as the

difference between ultimate strain and yield strain), post-yield strain energy, and toughness (27,29,30).

Bone material properties

The bone material properties were determined using nanoindentation. A bone core from each patient was embedded in epoxy and used to determine material level properties via nanoindentation. The embedded samples were ground, polished in diamond solutions with particle sizes of 3, 1, 0.25 and 0.05 µm (Buehler Eco Met 250 grinder and polisher) and abrasive papers of 1200, 2000 and 4000 grit sizes, under the water cooling condition. The samples were cleaned ultrasonically with distilled water between each polishing step.

Nanoindentation tests were performed using a TI-950 Tribo Indenter (Hysitron Inc., Minneapolis, MN, USA) with Berkovich pyramidal tip, having an included angle of 142.3° and tip radius of ~150 nm. The calibration of the instrument was performed using standard fused quartz and aluminum samples following the standard procedure (31,32). Locations for indents were identified using an in-situ scanning probe microscope integrated with the nanoindentation system. All tests were performed at room temperature in moist conditions.

Twenty (20) indents with a peak load of 3000 µN were applied to the longitudinal sections of the core(33). The load function consisted of a ten second ramp to peak force segment, followed by a thirty second hold and an unloading segment of ten second. The thirty-second hold time was adopted to eliminate creep effects (34). The load-displacement curves, obtained from indentation tests, were analyzed to determine the reduced modulus (Er) and hardness (H) (average of 20 indents) using Oliver and Pharr method in Triboscan (Hysitron) (35,36).

Composition

Thermogravimetric analyses (TGA) were performed to compare the bulk mineral-to-matrix ratio. Approximately 8 to 12 mg of trabecular bone underwent TGA analysis (TGA/DSC1 instrument, Mettler Toledo, Greifensee, Switzerland) in a controlled air atmosphere from room temperature to 1000 °C with a heating rate of 10°C/min. The thermal data were analyzed in STARe software (version 12.1). The mineral-to-matrix ratio was calculated as the ratio between the percentages of mass (% dry weight) remaining after heating to 600 °C and the organic mass loss between 200 °C and 600 °C. The protocol was adopted from published studies (37,38).

Mean crystal size

In order to obtain a powder, the half bone core was defatted and dehydrated in increasing concentrations of ethanol (70% to 100%) for 10 minutes each. The specimen was wet ground in acetone using mortar and pestle until a uniform and homogeneous powder was obtained [31]. X-ray diffraction (XRD) measurements were performed using CuKα radiation at 40 kV and 40 mA (X'Pert PRO, PANalytical) from 20 to 45° 2θ. The X'pert Highscore plus software was used for background correction and to fit the diffraction peaks at 2θ = 26° and 40° corresponding to 002 (c-axis direction) and 310 planes (ab-plane), respectively. The data of 002 and 310 planes were utilized to calculate the average length and width of mineral crystal respectively using the Scherrer equation(39–41).

Mineral and collagen properties

FTIR spectra were recorded from the freeze-dried bone section of donors using Bruker IFS 66v/S FTIR spectrophotometer in Attenuated Total Reflectance (ATR) mode, under the constant pressure, in the spectral region of 4000 to 400 cm^{-1} and used to calculate the following parameters: carbonate to phosphate ratio [area ratio of the carbonate ν2 peak (852-890 cm^{-1}) to phosphate ν1-ν3 peak (916-1180 cm^{-1})], mineral crystallinity [intensity ratio of 1030 cm^{-1} to 1020 cm^{-1}, which is related to crystal size and stoichiometric perfection], and the acid phosphate content [intensity ratio of 1127 cm^{-1} to 1096 cm^{-1}, which characterizes acid phosphate substitution into stoichiometric hydroxyapatite] (42,43). The Amide I band **(Figure 2B)** possesses structural information about the collagen matrix and is also the location of the strongest peaks for the non-enzymatic cross-link pentosidine (22)**.** Thus, sub-bands of the Amide I band were fitted with Gaussian curves at 1610, 1630, 1645, 1660, 1678 and 1692 cm^{-1} by using [a] peak analyzer tool in OriginPro 8.5 software. These peaks were chosen based on the second derivative approach**.** From the analysis of Amide I sub-bands, the non-enzymatic collagen crosslink-ratio (NE-xLR)(22) and enzymatic collagen cross-link ratio (E-xLR)(44) were measured through the area ratio of the 1678/1692 cm^{-1} and 1660/1678 cm^{-1} sub-bands, respectively. The measurement of NE-xLR enables the estimation of overall AGE content in bone tissue itself (22). Also, the collagen maturity [area ratio of 1660 cm^{-1} to 1690 cm^{-1}] was measured within the Amide I peak(44,45). The integrated area ratio (relative content) of Amide I and Amide II (46–48) bands were normalized with respect to methylene (CH_2) deformation band at 1450 cm^{-1}, similar to

previous studies (48,49). Finally, the mineral-to-matrix ratio [area ratio of the phosphate ν1-ν3 peak (916-1180 cm^{-1}) to amide I peak (1596-1712 cm^{-1})] was measured (42,43).

Fluorescent *Advanced Glycation End-products (fAGEs) assay*

Total fluorescent AGEs (fAGEs) were measured using fluorescence spectrometry and normalized to collagen concentration similar to previous studies(50,51). The 1/4th bone cores of each donor were lyophilized overnight then 45-55mg dried specimens were hydrolyzed in 6N HCl (100 µl/mg bone) at 110 °C for 20 h in hydrolysis vials with screw caps. The hydrolysate were cooled in room temperature, collected in a microcentrifuge tube, and centrifuged with 13000 rpm at 4°C (Eppendorf 5424R microcentrifuge). The supernatant is collected, diluted (ten times with DI water) and fluorescence were measured in a flat-bottom 96-well plate using a multi-mode microplate reader (CLARIOstar Plus, BMG LABTECH) at an excitation of 360 nm and an emission of 460 nm. The fluorescence data of specimens were normalized with serially diluted quinine standards (stock: 10 µg quinine per 1 mL of 0.1 N H_2SO_4) measured in the same way (50,51). Next, the absorbance assay of hydroxyproline was performed to determine collagen content to normalize the total fluorescence(50). Total fAGEs are reported in units of ng quinine fluorescence/mg collagen. The collagen content is derived based on prior knowledge that collagen consists of 14% hydroxyproline (52). All solutions used were freshly prepared, and experiments were performed in darkness at room temperature.

Statistical Analysis

Distributions of mechanical properties were plotted to identify potential outliers, and the data from five donors (three from the non-diabetic group and two from the diabetic group) with values two standard deviations beyond the mean were removed from all analysis. The distribution of the data was tested for normality by the Kolmogorov-Smirnov test. Homogeneity of variances was analyzed using Levene's test. Between-group differences of calculated parameters were analyzed for statistical significance using Student's t-tests, after testing for normality and homogeneity of variances. Mean values and standard deviation were calculated for the measured parameters. Pearson correlation tests were used to determine relationships between variables. Forward stepwise regression tests were conducted for mechanical properties using all significant parameters as independent variables. An analysis

of covariance (ANCOVA) was conducted to compare the differences in mechanical properties among groups by using BV/TV as a covariate. Post-hoc power calculation was performed by comparing the mean value of post-yield energy and toughness between diabetic and non-diabetic groups using an ANOVA test. A confidence level of $p < 0.05$ implies a statistical significance between the groups where $p<0.05$, $p<0.01$ and $p<0.001$ denote the level of significance. Statistical analysis was performed using SPSS (v.21, SPSS Inc., Chicago, IL, USA) and Microsoft Office Excel (2007).

RESULTS

Patient characteristics

Table 1 shows the baseline characteristics of patients with diabetes (n=30) and without diabetes (n=40). The mean age of the diabetic and non-diabetic group was 69.7±10.0 and 69.8±10.2 years, respectively. The sex distribution among groups was also similar. Other than pre-operative glycosylated hemoglobin A1c (HbA1c) levels, no significant differences were observed in other baseline characteristics, including aBMD, T score, and biochemical parameters between diabetic and non-diabetic groups. The duration of diabetes ranges from 4 to15 (7.5±2.8) years.

Microstructural parameters

Representative µ-CT images and map of trabecular thickness in diabetic and non-diabetic bones are shown in (**Figure 3),** and the mean values of microstructural parameters are shown in **Table 2**. The diabetic group had significantly lower BV/TV (14.21%, **p = 0.03**), Tb.Th (mm) (10.8%, **p = 0.019**), and Tb.N (1/mm) (8.0%, **p = 0.033**), higher Tb.Sp (mm) (12.27%, p = 0.095) and structure model index (SMI) (24.48%, **p = 0.037**) compared to the non-diabetic group. We observed similar mean values (p=0.475) of degree of anisotropy (DA) among both groups. The mean value of SMI for the diabetic and non-diabetic groups is 2.39 ± 0.19 and 1.92 ± 0.12, respectively **(p=0.037)**, indicating that the rod-like trabeculae structure is dominant in the diabetic group, compared to non-diabetics.

Mechanical properties

The mean values of modulus, yield stress, ultimate stress, yield strain, ultimate strain, post-yield strain, post-yield energy, and toughness for both groups are shown in (**Figure 3 E-L)**. The modulus, yield stress, ultimate stress, post-yield energy and toughness were found to be lower by 25% (**p=0.03**), 27% (**p=0.01**), 25% (**p=0.02**), 47% (**p=0.007**) and 45% (**p=0.005**), respectively in the diabetic group as compared to the non-diabetic group. These results indicate that the load-bearing and energy absorption capacity is significantly compromised in the diabetic bone. However, yield strain, ultimate strain, and post-yield strain did not differ across groups.

Material properties

Nanoindentation tests for both the groups reveal that under the same load of 3000 µN, the diabetic group had significantly lower values of modulus (7.37±2.96 GPa to 9.0±2.7 GPa, **p=0.033**) and hardness (0.294±0.150 GPa to 0.444±0.152 GPa, **p=0.014**) than the non-diabetic group. The modulus and hardness were found to be lower by 18.1% and 33.8%, respectively in the diabetic group as compared to the non-diabetic group (**Figure 4 A-B)**.

Composition

Representative thermo-gravimetric analysis (TGA) curves of weight (%) vs temperature with their respective first derivatives are plotted in **(Figure 4C)**. The percentage of weight associated with water content [m24°C (%) – m200°C (%)], organic content [m200°C (%) – m600°C (%)], mineral content [m600°C (%) / m200°C (%)] and carbonate content [m600°C (%) – m800°C (%)] are shown in **Table 2**. Diabetic bones exhibited decreased mineral content **(p=0.038)** compared with non-diabetics. No significant differences are found in the organic content (p=0.087), water content (p=0.335) and carbonate content (p= 0.988). Mineral/matrix ratio indicate that diabetic bones had lower mineral/matrix ratio compared with non-diabetics **(p = 0.016)** as shown in **(Figure 4D)**.

Mean mineral crystal size

The representative XRD pattern of trabecular bone is shown in (**Figure 5A)**. The mean crystal length was not different between the groups (**Figure 5B)**, whereas diabetic bone had significantly larger crystal width than the non-diabetic bones (8.12±2.07 nm *vs* 6.57±1.33 nm, **p=0.024**) as shown in **(Figure 5C)**.

Mineral and collagen properties

The representative FTIR spectra of bone with the appropriate label of various bands and schematic presentation of enzymatic and non-enzymatic collagen cross-links are shown in **(Figure 6 A-C).** The mineral-based parameters including mineral crystallinity (p=0.073), carbonate/phosphate ratio (p=0.58), and acid phosphate content (p=0.84) were not significantly different between the groups (**Figure 6 D-F)**.

The collagen cross-links [NE-xLR (area ratio of 1678/1692 cm^{-1} sub-bands), E-xLR (area ratio of 1660/1678 cm^{-1} sub-bands)] and collagen maturity (area ratio of 1660/1690 cm^{-1}) are shown in (**Figure 6 G-I)**. The diabetic bone had significantly higher NE-xLR [by 46.6%, **p=0.008]** and lower E-xLR [by 35%, **p=0.032]** compared to the non-diabetic bone, whereas no significant difference was observed in collagen maturity. Further, the diabetic bone had lower mineral/matrix ratio [by 21.1%, (**p=0.046**)] as shown in (**Figure 6J)**.

Table 2 shows the shift in the position of Amide I **(p = 0.02)** and Amide II **(p = 0.009) bands**. The diabetic group had a lower value of area under the normalized peaks of Amide I and Amide II bands by 47.36% **(p< 0.001)** and 52.4% **(p<0.001)**, respectively, compared to the non-diabetic group. These results indicate that the secondary structure of Amide I and Amide II proteins is altered and the quantity of these proteins is lower in the diabetic bone.

Florescent advanced glycation endproducts (fAGEs)

The diabetic bone had 32.1% higher fAGEs concentration than the non-diabetic bone (443 ± 198 vs. 335 ±155 ng quinine/mg collagen, **p=0.015**) as reported in (**Figure 7A).**

Interrelationships between variables

Pre-operative HbA1c was positively correlated with fAGEs (r=0.635, p<0.001) and NE-xLR (r=0.561, p=0.006). Correlations between HbA1c and mechanical properties revealed that within diabetic group, HbA1c is significantly and negatively correlated with post-yield energy (r=-0.402, p=0.047), whereas this relationship was not significant in the non-diabetic group**.** Other than the reported parameters, none of the parameters were correlated with HbA1c. Furthermore, fAGEs were negatively correlated with mineral/matrix ratio (r=-0.487, p=0.016), BV/TV (r=-0.488, p=0.021), Tb.Th (r=-0.454, p=0.044), and positively correlated with NE-xLR (r=0.367, p=0.045). The fAGEs were also negatively correlated with mechanical properties including post-yield energy (r=-0.489, **p=0.013**), and toughness (r=-0.441, **p=0.027**) in the diabetic group as shown in (**Figure 7 B-C)**. Additionally, the NE-xLR was negatively correlated with the post-yield strain (r=-0.433, **p=0.031**) in diabetic but not in the non-diabetic group as shown in (**Figure 7D)**. The detailed correlation analysis of selected significant variables is reported in **Table 3** and **Table 4** for diabetic and non-diabetic groups, respectively.

ANCOVA analysis comparing the effect of change in BV/TV on the change in mechanical properties between groups demonstrated that both regression slopes and intercept for modulus, yield stress and ultimate stress were similar between groups as shown in (**Figure 8 A-C),** respectively. The regression slopes of post-yield energy (p=0.792) and toughness (p=0.977) were also similar between groups, whereas the intercept was significantly lower in diabetic group for these properties (**p=0.028**) and (**p=0.032**) (**Figure 8 D-E)**. These results reveal that the magnitude of change in BV/TV does not account for the differences in post-yield properties observed between the two groups.

Forward stepwise regression tests to predict mechanical properties as a dependent variable using all significant parameters as independent variables showed that in the diabetic group the BV/TV, fAGEs and mineral-to-matrix ratio (FTIR) can explain up to 86.7% (**p<0.001**) of variance in ultimate strength, whereas in the non-diabetic group, only BV/TV was observed to be a significant predictor explaining up to 39.8% of the variance in ultimate strength. Mineral-to-matrix ratio (FTIR) and Tb.Th were found to predict yield strain up to 77.4% (**p<0.001**) in the diabetic group.

The power of study was performed by comparing the mean value of post-yield energy and toughness between diabetic and non-diabetic groups, this outcome were found to be 88% and

82% respectively.

DISCUSSION

This is the first investigation linking biomechanical, microstructural, material and compositional properties of human bone in individuals with diabetes and known fragility fractures. Our findings provide evidence of detrimental effects of hyperglycemia on trabecular bone quality at multiple organizational scales leading to lower energy absorption and toughness, which can explain the increased bone fragility in patients with T2D.

The overall loss in bone quality and strength may be governed by a cascade of events happening at different length scales, such as abnormalities in the mineral and collagen quality at the nanoscale, accumulation of unrepaired microdamage or microcracks at the microscale, and changes in the trabecular architecture and a decrease in the trabecular connectivity at the mesoscale. Furthermore, any alteration in the properties locally, either at micro- or nano-level, affects the properties of the hierarchical organization of bone at higher scales (53,54). Thus, our findings of differences at nanoscale and microscale can be linked to each other and to higher scales to get a comprehensive diagnosis of altered bone quality and fracture risk in diabetes. To this end, forward stepwise regression analysis of multiscale data, presented here, shows that the BV/TV, fAGE and mineral-to-matrix ratio (FTIR) can explain up to 86.7% of the variance in ultimate strength. Also, the mineral-to-matrix ratio (FTIR) and Tb.Th together can explain up to 77.4% of the variance in yield strain. Thus, in addition to bone microstructure (BV/TV, Tb.Th), nanoscale characteristics of bone (mineral-to-matrix ratio) and collagen quality (fAGEs) are important predictors of the loss in mechanical properties and the associated increase in fracture risk of diabetic bone.

Particularly, the assessment of bone microstructure with micro CT showed lower BV/TV (%) in diabetics when compared to the non-diabetics. Moreover, the structure was noticeably altered, evidenced by the thinning of trabeculae and, in general, by fewer trabeculae. Indeed, due to this compromised bone microstructure, a lower value of ultimate stress (uniaxial compression) is observed in those with diabetes. The results of uniaxial compression tests found in our study are consistent with previously published studies (55–59). Our results of microstructural parameters are slightly different from those reported in earlier studies (10,11,13). However, in these studies bone tissue was obtained from individuals with obisity and/or severe arthritis which could explain their findings of same or

increased BV/TV in those compared with diabetes. It is also possible that our study finding of lower BV/TV in diabetes is related to the distinct phenotypes of Asians (19,60–64).

At the apparent-level (uniaxial-compression) and tissue level (nanoindentation), the lower value of modulus (stiffness), observed with the diabetic bone, are directly associated with decreased mineral-to-matrix ratio (FTIR). The wider crystal size without a change in length decreases the aspect ratio (surface area/volume) of apatite crystals and explains reduced elastic modulus of bone material (65). Furthermore, altered crystal shape also can affect crystal connectivity, orientation, and arrangement (65).

We also observed the increase in protein misfolding (altered secondary structure of proteins) and a decrease in relative protein content (Amide I and Amide II) in the diabetic bone. The altered secondary structure is primarily responsible for the change in the structural integrity of the collagen in bone (66). This altered collagen structure can change the hydration level of collagen, and/or change in shape, size, orientation, and growth of inorganic mineral content (67) as noted above.

One of the reasons for the degradation of bone quality in diabetes could be prolonged hyperglycemia (HbA1c) which may increase the accumulation of AGEs in the bone matrix. In correlation analysis, we found the HbA1c is positively correlated with fAGEs content and NE-xLR. We also observed the reduced enzymatic collagen cross-link ratio (E-xLR) and increased non-enzymatic collagen cross-link ratio (NE-xLR) in the diabetic group as compared to the non-diabetic group. The enzymatic cross-links (E-xL, beneficial cross-links) are responsible for mechanical strength whereas NE-xL is associated with bone fragility (68–70). Our findings of reduced E-xLR and increased NE-xLR are evidence of AGE accumulation (NE-xL) in the bone, which induces tissue damage through structural modification of proteins and abnormal collagen fibril organization in the diabetic bone. The reduction of E-xLR can be associated with hyperglycemia and oxidative stress (OS) (71,72). Further, the NE-xL (AGE accumulation) in diabetic bone favors material rigidity by restricting the uncoiling of the triple helical structure of collagen (flexibility) and confining the natural energy dissipation process during loading to a limited region (73). Such changes will alter the nature of microdamage formation in bone from diffuse cracking, characteristic of ductile materials, to linear microcracks, making bone more susceptible to the fracture (69,74,75). Indeed, in the present study, elevated levels of HbA1c, fAGEs, and NE-xLR correlated negatively with bone biomechanical properties – post-yield energy, toughness, and post-yield strain in diabetes. Also, the lower value of intercept of post-yield energy and toughness in diabetic group (ANCOVA) revealed that the glycated bone exhibited lesser

energy dissipation and reduced toughness. Our results are consistent with previously published studies that reported the accumulation of AGEs as a cause for abnormal collagen synthesis and altered collagen structure (76) in the bone. Thus, changes in collagen, mineral, altered bone composition at the nanoscale, and lower bone volume fraction and trabecular architecture at the microscale in diabetic group provides detailed insight on skeletal fragility in diabetes and improves the current understanding on the impact of diabetes on bone homeostasis.

In the present study, FN BMD T-scores were similar among those with T2D and without diabetes. The deficits in bone quality in T2D mentioned above underlie the compromised bone strength in diabetes. These findings explain the inability of BMD T-score, a quantitative measure, to accurately predict fracture risk in T2D as previously reported in large studies (4,77). In the Study of Osteoporotic Fractures (4), for a given age and T-score, the risk of hip or non-spine fracture was higher in women with T2D than those without diabetes after 25 years of follow up. While T-score is useful in fracture risk assessment in women with and without diabetes, however T-score underestimates fracture risk in T2D (4,9).

Various techniques (pQCT, HRpQCT, Osteoprobe) have been used in research to investigate bone quality and bone strength. However, each technique presents its own challenges for utilization in routine clinical practice. In MrOS (77), pQCT was used to assess bone strength at peripheral sites in T2D and lower bone bending strength was observed at mid shaft regions of radius and tibia in those with T2D, despite no differences in cortical vBMD. Though pQCT is a clinically available tool, the imaging resolution remains a limitation. Consequently, various approaches have been proposed to include changes in bone quality and explain poor bone mechanical properties, such as those reported here. For example, bone strength estimated by micro-finite element analysis (micro-FEA/HR-pQCT) at the distal radius has been shown to be lower in T2D compared to controls (78). Similarly, micro-indentation of the tibial cortex has been performed to demonstrate that the estimated bone material strength index (BMSi) is decreased in T2D compared to controls (79–81). While these techniques have increased our understanding of bone fragility in diabetes, further work is needed to assess their application for routine clinical use. The only tool currently approved for clinical assessment of bone quality is trabecular bone score (TBS) (5,82) which help to predict fracture risk, independent of BMD. However, TBS is a surrogate measurement of trabecular architecture and not a tool for assessment of bone strength. Hence, diagnostic tools are needed for specific and direct assessment of bone quality to aid clinical assessment

of fracture risk in diabetes. Meanwhile, the International Osteoporosis Foundation (IOF) recommends adjusting BMD T-score for diabetes to avoid underestimation of risk in clinical practice (9).

This study has some limitations. First, this study is limited to *ex vivo* assessments of bone quality in patients who underwent hip fragility fractures. Non-fracture controls with and without diabetes were not studied, however it is not feasible to obtain femoral head specimen from healthy controls. Second, the study focuses exclusively on trabecular bone and does not include properties of cortical bone. Other studies have reported the increased cortical porosity (6,12,78) and altered cortical bone material properties *in vivo*, by demonstratingdecreased BMSi (measured through Osteoprobe) in those with diabetes compared to controls (79,80,83). Also, the study lacks information on the effect of type of diabetes treatment (insulin, metformin, and other anti-diabetic treatment) on bone properties. Sample sizes within each subgroup are small, and a large randomized clinical trial would be necessary to draw any meaningful conclusion regarding the effect of diabetes treatment on bone properties. Further, we could not assess bone remodeling via dynamic bone labeling. Lastly, we used femoral head specimens instead of femoral neck (typical fracture site) because in most cases of fracture, femoral necks are extensively and variably damaged either due to fracture or during surgery. Thus, it was difficult to obtain uniform specimens from all patients. Hence to avoid site-specific differences, we took samples from the femoral head.

Despite the above-mentioned limitations, our study's major strength is that the explants characterized here are from the patients with diabetes with known fragility fractures. Further, this study includes a wide range of duration and severity of the disease and this is an important and unique aspect of our study because longer duration of diabetes is typically required for skeletal changes in diabetes to fully manifest. The severity and duration of diabetes are known to greatly affect fracture risk (6,84) and therefore it may also affect the degree of compositional changes. This aspect could also explain the differences between fAGEs results in our study and those reported in other studies (10,11) where a significant difference in fAGEs was not observed between groups. One study (10) included samples for a shorter duration of disease of nearly two years, whereas in other study (11), the information on duration of diabetes was not reported. The results of our fAGEs content are consistent with one recent study (13) that found a 1.5-fold increase in fAGEs content in women with T2D of mean duration of nearly15 years compared with non-diabetic women.

In conclusion, the study findings provide evidence that diabetes affects the trabecular bone quality at multiple organization levels. The accumulation of AGEs is one of the processes that favor deterioration of bone quality in diabetes leading to material, structural, compositional, and biomechanical dysfunctionality. Overall, together with altered structure and material properties, these novel findings of changes in the composition of bone explain the compromised mechanical performance and diminished bone strength in diabetes. Finally, this study demonstrates that whilst osteoporotic bones are fracture prone, diabetes is detrimental to bone quality, thus highlighting the need for more specific measures to understand and diagnose bone quality and bone fragility in T2D.

Acknowledgments:

The IIT Ropar and PGIMER Chandigarh are acknowledged for providing the infrastructure and facilities used in the current research. The Department of Science and Technology, India (CRG/2018/002219) and IMPRINT - Ministry of Human Resource Development, India (IMP/2019/000150) are acknowledged for providing the necessary funds. The authors acknowledge Mr. Aakash Soni for his help in editing the manuscript for grammar and proofreading. The authors acknowledge Dr. Atharva Poundarik for his help in statistical analysis at multiscale and intellectual discussion during the preparation of manuscript.

Contributions

P.S. designed the experiments, conducted experiments, analyzed and interpreted the data, and wrote the manuscript, R.N.Y. designed the micro-CT and Uniaxial compression experiments, performed experiments and analyzed the data, V.D., J.C.B., D.N., S.K. were involved in all data collection, S.S., S.A., V.G.G., did data collection, data interpretation and revising the manuscript content, V.M. revised the manuscript content, DV provided input on multiscale analysis of data, interpretation of results and edited the manuscript; R.D. provided clinical expertise, input on interpretation of results and edited the manuscript, S.K.B, and N.K. identified the research problem and supervised the entire work in every step.

Data Availability The datasets generated during and/or analyzed during the current study are available from the corresponding authors on reasonable request.

References

1. **Palermo A, D'Onofrio L, Eastell R, Schwartz A V., Pozzilli P, Napoli N.** Oral anti-diabetic drugs and fracture risk, cut to the bone: safe or dangerous? A narrative review. *Osteoporos. Int.* 2015;26(8):2073–2089.

2. **Karim L, Rezaee T, Vaidya R.** The Effect of Type 2 Diabetes on Bone Biomechanics. *Curr. Osteoporos. Rep.* 2019. doi:10.1007/s11914-019-00526-w.

3. **Janghorbani M, Van Dam RM, Willett WC, Hu FB.** Systematic review of type 1 and type 2 diabetes mellitus and risk of fracture. *Am. J. Epidemiol.* 2007;166(5):495–505.

4. **Schwartz A V., Vittinghoff E, Bauer DC, Hillier TA, Strotmeyer ES, Ensrud KE, Donaldson MG, Cauley JA, Harris TB, Koster A, Womack CR, Palermo L, Black DM.** Association of BMD and FRAX score with risk of fracture in older adults with type 2 diabetes. *JAMA - J. Am. Med. Assoc.* 2011;305(21):2184–2192.

5. **Dhaliwal R, Cibula D, Ghosh C, Weinstock RS, Moses AM.** Bone quality assessment in type 2 diabetes mellitus. *Osteoporos. Int.* 2014;25(7):1969–1973.

6. **Patsch JM, Burghardt AJ, Yap SP, Baum T, Schwartz A V., Joseph GB, Link TM.** Increased cortical porosity in type 2 diabetic postmenopausal women with fragility fractures. *J. Bone Miner. Res.* 2013;28(2):313–324.

7. **Linde JS, Hygum K, Langdahl BL.** Skeletal Fragility in Type 2 Diabetes Mellitus. *Endocrinol. Metab.* 2018;33(3):339–351.

8. **Farr JN, Khosla S.** Determinants of bone strength and quality in diabetes mellitus in humans. *Bone* 2016;82:28–34.

9. **Ferrari SL, Abrahamsen B, Napoli N, Akesson K, Chandran M, Eastell R, El-Hajj Fuleihan G, Josse R, Kendler DL, Kraenzlin M, Suzuki A, Pierroz DD, Schwartz A V., Leslie WD, Ferrari SL, Ardawi MSM, Cooper C, Mithal A.** Diagnosis and management of bone fragility in diabetes: an emerging challenge. *Osteoporos. Int.* 2018;29(12):2585–2596.

10. **Karim L, Moulton J, Van Vliet M, Velie K, Robbins A, Malekipour F, Abdeen A, Ayres D, Bouxsein ML.** Bone microarchitecture, biomechanical properties, and advanced glycation end-products in the proximal femur of adults with type 2 diabetes.

Bone 2018. doi:https://doi.org/10.1016/j.bone.2018.05.030.

11. **Hunt HB, Torres AM, Palomino PM, Marty E, Saiyed R, Cohn M, Jo J, Warner S, Sroga GE, King KB, Lane JM, Vashishth D, Hernandez CJ, Donnelly E.** *Altered Tissue Composition, Microarchitecture, and Mechanical Performance in Cancellous Bone From Men With Type 2 Diabetes Mellitus*.; 2019. doi:10.1002/jbmr.3711.

12. **Wölfel; EM, Jähn-Rickert K, Schmidt FN, Wulff B, Mushumba H, Sroga GE, Püschel K, Milovanovic P, Amling M, Campbell GM, Vashishth D, Busse B.** Individuals with type 2 diabetes mellitus show dimorphic and heterogeneous patterns of loss in femoral bone quality. *Bone* 2020:125871.

13. **Piccoli A, Cannata F, Strollo R, Pedone C, Leanza G, Russo F, Greto V, Isgrò C, Quattrocchi CC, Massaroni C, Silvestri S, Vadalà G, Bisogno T, Denaro V, Pozzilli P, Tang SJ, Silva MJ, Conte C, Papalia R, Maccarrone M, Napoli N.** Sclerostin Regulation, Microarchitecture, And Advanced Glycation End- Products In The Bone Of Elderly Women With Type 2 Diabetes. *J. Bone Miner. Res.* 2020. doi:10.1002/jbmr.4153.

14. **Gallant MA, Brown DM, Organ JM, Allen MR, Burr DB.** Reference-point indentation correlates with bone toughness assessed using whole-bone traditional mechanical testing. *Bone* 2013;53(1):301–305.

15. **Rubin MR, Paschalis EP, Poundarik A, Sroga GE, McMahon DJ, Gamsjaeger S, Klaushofer K, Vashishth D.** Advanced Glycation Endproducts and Bone Material Properties in Type 1 Diabetic Mice. Geoffroy V, ed. *PLoS One* 2016;11(5):e0154700.

16. **Marin C, Papantonakis G, Sels K, Van Lenthe GH, Falgayrac G, Vangoitsenhoven R, Van Der Schueren B, Penel G, Luyten F, Vandamme K, Kerckhofs G.** Unraveling the compromised biomechanical performance of type 2 diabetes- and Roux-en-Y gastric bypass bone by linking mechanical-structural and physico-chemical properties. *Sci. Rep.* 2018;8(1):1–12.

17. **Acevedo C, Sylvia M, Schaible E, Graham JL, Stanhope KL, Metz LN, Gludovatz B, Schwartz A V., Ritchie RO, Alliston TN, Havel PJ, Fields AJ.** Contributions of Material Properties and Structure to Increased Bone Fragility for a Given Bone Mass in the UCD-T2DM Rat Model of Type 2 Diabetes. *J. Bone Miner. Res.*

2018;33(6):1066–1075.

18. **Hunt HB, Pearl JC, Diaz DR, King KB, Donnelly E.** Bone Tissue Collagen Maturity and Mineral Content Increase With Sustained Hyperglycemia in the KK-Ay Murine Model of Type 2 Diabetes. *J. Bone Miner. Res.* 2018;33(5):921–929.

19. **Sihota P, Yadav RN, Poleboina S, Mehandia V, Bhadada SK, Tikoo K, Kumar N.** Development of HFD - fed/low dose STZ treated female Sprague Dawley rat model to investigate diabetic bone fragility at different organization levels . *JBMR Plus* 2020. doi:10.1002/jbm4.10379.

20. **Thomas CJ, Cleland TP, Sroga GE, Vashishth D.** Accumulation of carboxymethyl-lysine (CML) in human cortical bone. *Bone* 2018;(Cml). doi:10.1016/j.bone.2018.01.028.

21. **Gkogkolou P, Bohm M, Böhm M.** Advanced glycation end products: key players in skin ageing? *Gkogkolou, Paraskevi Bohm, Markus* 2012;4(3):259–270.

22. **Schmidt FN, Zimmermann EA, Campbell GM, Sroga GE, Püschel K, Amling M, Tang SY, Vashishth D, Busse B.** Assessment of collagen quality associated with non-enzymatic cross-links in human bone using Fourier-transform infrared imaging. *Bone* 2017;97:243–251.

23. **Burr DB.** Full Length Article: Changes in bone matrix properties with aging. *Bone* 2019;120(September 2018):85–93.

24. **American Diabetes Association (ADA).** Standard of medical care in diabetes - 2017. *Diabetes Care* 2017;40 (sup 1)(January):s4–s128.

25. **Doube M, Klosowski MM, Arganda-Carreras I, Cordelières FP, Dougherty RP, Jackson JS, Schmid B, Hutchinson JR, Shefelbine SJ.** BoneJ: Free and extensible bone image analysis in ImageJ. *Bone* 2010;47(6):1076–1079.

26. **Bouxsein ML, Boyd SK, Christiansen BA, Guldberg RE, Jepsen KJ, Müller R.** Guidelines for assessment of bone microstructure in rodents using micro-computed tomography. *J. Bone Miner. Res.* 2010;25(7):1468–1486.

27. **Wang J, Zhou B, Liu XS, Fields AJ, Sanyal A, Shi X, Adams M, Keaveny TM, Guo XE.** Trabecular plates and rods determine elastic modulus and yield strength of human trabecular bone. *Bone* 2015;72:71–80.

28. **Zdero R.** *Experimental methods in orthopaedic biomechanics*.; 2017.

29. **An YH, Draughn RA.** Mechanical testing of bone and the bone implant interface. 2000:624.

30. **Karim L, Vashishth D.** Heterogeneous glycation of cancellous bone and its association with bone quality and fragility. *PLoS One* 2012;7(4). doi:10.1371/journal.pone.0035047.

31. **Bhushan B.** Depth-sensing nanoindentation measurement techniques and applications. *Microsyst. Technol.* 2017;23(5):1595–1649.

32. **Saini K, Discher D, Kumar N.** Static and time-dependent mechanical response of organic matrix of bone. *J. Mech. Behav. Biomed. Mater.* 2019;91(December 2018):315–325.

33. **Edward Hoffler C, Edward Guo X, Zysset PK, Goldstein SA.** An application of nanoindentation technique to measure bone tissue lamellae properties. *J. Biomech. Eng.* 2005;127(7):1046–1053.

34. **Rodriguez-florez N, Oyen ML, Shefelbine SJ, Pharr O.** Insight into differences in nanoindentation properties of bone. *J. Mech. Behav. Biomed. Mater.* 2013;18:90–99.

35. **Oliver WC, Pharr GM.** An improved technique for determining hardness and elastic modulus using load and displacement sensing indentation experiments. *J. Mater. Res.* 1992;7(06):1564–1583.

36. **Das R, Kumar A, Patel A, Vijay S, Saurabh S, Kumar N.** Biomechanical characterization of spider webs. *J. Mech. Behav. Biomed. Mater.* 2017;67(September 2016):101–109.

37. **Rodriguez-Florez N, Garcia-Tunon E, Mukadam Q, Saiz E, Oldknow KJ, Farquharson C, Millán JL, Boyde A, Shefelbine SJ.** An investigation of the mineral in ductile and brittle cortical mouse bone. *J. Bone Miner. Res.* 2015;30(5):786–795.

38. **Mkukuma LD, Imrie CT, Skakle JMS, Hukins DWL, Aspden RM.** Thermal stability and structure of cancellous bone mineral from the femoral head of patients with osteoarthritis or osteoporosis. *Ann. Rheum. Dis.* 2005;64(2):222–225.

39. **Farlay D, Panczer G, Rey C, Delmas PD, Boivin G.** Mineral maturity and

crystallinity index are distinct characteristics of bone mineral. *J. Bone Miner. Metab.* 2010;28(4):433–445.

40. **Turunen MJ, Kaspersen JD, Olsson U, Guizar-Sicairos M, Bech M, Schaff F, Tägil M, Jurvelin JS, Isaksson H.** Bone mineral crystal size and organization vary across mature rat bone cortex. *J. Struct. Biol.* 2016;195(3):337–344.

41. **Vetter U, Eanes ED, Kopp JB, Termine JD, Robey PG.** Changes in apatite crystal size in bones of patients with osteogenesis imperfecta. *Calcif. Tissue Int.* 1991;49(4):248–250.

42. **Boskey A, Mendelsohn R.** Infrared analysis of bone in health and disease. *J. Biomed. Opt.* 2005;10(3):31102.

43. **Spevak L, Flach CR, Hunter T, Mendelsohn R, Boskey AL.** FTIRI Parameters describing Acid Phosphate Substitution in Biologic Hydroxyapatite. *Calcif. Tissue Int.* 2013;92(5):418–428.

44. **Paschalis EP, Gamsjaeger S, Tatakis DN, Hassler N, Robins SP, Klaushofer K.** Fourier transform infrared spectroscopic characterization of mineralizing type i collagen enzymatic trivalent cross-links. *Calcif. Tissue Int.* 2014;96(1):18–29.

45. **Farlay D, Duclos ME, Gineyts E, Bertholon C, Viguet-Carrin S, Nallala J, Sockalingum GD, Bertrand D, Roger T, Hartmann DJ, Chapurlat R, Boivin G.** The ratio 1660/1690 cm-1 measured by infrared microspectroscopy is not specific of enzymatic collagen cross-links in bone tissue. *PLoS One* 2011;6(12). doi:10.1371/journal.pone.0028736.

46. **Bozkurt O, Severcan M, Severcan F.** Diabetes induces compositional, structural and functional alterations on rat skeletal soleus muscle revealed by FTIR spectroscopy: a comparative study with EDL muscle. *Analyst* 2010;135(12):3110.

47. **Gu C, Katti DR, Katti KS.** Microstructural and Photoacoustic Infrared Spectroscopic Studies of Human Cortical Bone with Osteogenesis Imperfecta. *Jom* 2016;68(4):1116–1127.

48. **Sihota P, Yadav RN, Dhiman V, Bhadada SK, Mehandia V, Kumar N.** Investigation of diabetic patient's fingernail quality to monitor type 2 diabetes induced tissue damage. *Sci. Rep.* 2019;9(1):3193.

49. **Towler MR, Wren A, Rushe N, Saunders J, Cummins NM, Jakeman PM.** Raman spectroscopy of the human nail: A potential tool for evaluating bone health? *J. Mater. Sci. Mater. Med.* 2007;18(5):759–763.

50. **Poundarik AA, Wu PC, Evis Z, Sroga GE, Ural A, Rubin M, Vashishth D.** A direct role of collagen glycation in bone fracture. *J. Mech. Behav. Biomed. Mater.* 2015;52:120–130.

51. **Sroga GE, Siddula A, Vashishth D.** Glycation of human cortical and cancellous bone captures differences in the formation of maillard reaction products between glucose and ribose. *PLoS One* 2015;10(2):1–19.

52. **Eastoe JE.** The amino acid composition of mammalian collagen and gelatin. *Biochem. J.* 1955;61(4):589–600.

53. **Rai RK, Sinha N.** Dehydration-induced structural changes in the collagen-hydroxyapatite interface in bone by high-resolution solid-state NMR spectroscopy. *J. Phys. Chem. C* 2011;115(29):14219–14227.

54. **Sabet FA, Najafi AR, Hamed E, Jasiuk I.** Modelling of bone fracture and strength at different length scales: A review. *Interface Focus* 2016;6(1):20–30.

55. **Lv H, Zhang L, Yang F, Zhao Z, Yao Q, Zhang L, Tang P.** Comparison of microstructural and mechanical properties of trabeculae in femoral head from osteoporosis patients with and without cartilage lesions: A case-control study Pathophysiology of musculoskeletal disorders. *BMC Musculoskelet. Disord.* 2015;16(1):1–10.

56. **Aleixo I, Vale AC, Lúcio M, Amaral PM, Rosa LG, Caetano-Lopes J, Rodrigues A, Canhão H, Fonseca JE, Vaz MF.** A method for the evaluation of femoral head trabecular bone compressive properties. *Mater. Sci. Forum* 2013;730–732(January):3–8.

57. **Wolfram U, Wilke HJ, Zysset PK.** Damage accumulation in vertebral trabecular bone depends on loading mode and direction. *J. Biomech.* 2011;44(6):1164–1169.

58. **Giulia M, Alessio D, Gabriela C, Massimo L, Chiara N, Marco C, Nicola B, Fabrizio G, Sonia F, Chiara VB.** Osteoporosis-related variations of trabecular bone properties of proximal human humeral heads at different scale lengths. *J. Mech. Behav.*

Biomed. Mater. 2019;100(April):103373.

59. **Hambli R.** Micro-CT finite element model and experimental validation of trabecular bone damage and fracture. *Bone* 2013;56(2):363–374.

60. **Walsh JS, Vilaca T.** Obesity, Type 2 Diabetes and Bone in Adults. *Calcif. Tissue Int.* 2017;100(5):528–535.

61. **Cho YM.** Characteristics of the pathophysiology of type 2 diabetes in Asians. *Ann. Laparosc. Endosc. Surg.* 2017;2:14–14.

62. **Chan JCN, Yeung R, Luk A.** The Asian diabetes phenotypes: Challenges and opportunities. *Diabetes Res. Clin. Pract.* 2014;105(1):135–139.

63. **Fukushima M, Usami M, Ikeda M, Nakai Y, Taniguchi A, Matsuura T, Suzuki H, Kurose T, Yamada Y, Seino Y.** Insulin secretion and insulin sensitivity at different stages of glucose tolerance: A cross-sectional study of Japanese type 2 diabetes. *Metabolism.* 2004;53(7):831–835.

64. **Matsumoto K, Miyake S, Yano M, Ueki Y, Yamaguchi Y, Akazawa S, Tominaga Y.** Glucose tolerance, insulin secretion, and insulin sensitivity in nonobese and obese Japanese subjects. *Diabetes Care* 1997;20(10):1562–1568.

65. **Maximilien Vanleene, Porter A, Guillot P-V, Boyde A, Oyen M, Shefelbine S.** Ultra-structural defects cause low bone matrix stiffness despite high mineralization in osteogenesis imperfecta mice. *Bone* 2012;50(6):1317–1323.

66. **Napoli N, Chandran M, Pierroz DD, Abrahamsen B, Schwartz A V., Ferrari SL, Group O behalf of the IB and DW.** Mechanisms of diabetes mellitus-induced bone fragility. *Nat. Rev. Endocrinol.* 2016;13(4):208–219.

67. **Rai RK, Singh C, Sinha N.** Predominant role of water in native collagen assembly inside the bone matrix. *J. Phys. Chem. B* 2015;119(1):201–211.

68. **Saito M, Kida Y, Kato S, Marumo K.** Diabetes, collagen, and bone quality. *Curr. Osteoporos. Rep.* 2014;12(2):181–188.

69. **Saito M, Marumo K.** Collagen cross-links as a determinant of bone quality: A possible explanation for bone fragility in aging, osteoporosis, and diabetes mellitus. *Osteoporos. Int.* 2010;21(2):195–214.

70. **Viguet-Carrin S, Garnero P, Delmas PD.** The role of collagen in bone strength. *Osteoporos. Int.* 2006;17(3):319–336.

71. **Min-Xin Fu, Jesus R. Requena, Alicia J. Jenkins, Timothy J. Lyons, John W. Baynes and SRT.** The Advanced Glycation End Product, N -(Carboxymethyl)lysine, Is a Product of both Lipid Peroxidation and Glycoxidation Reactions. *J. Biol. Chem.* 2002;271(17):9982–9986.

72. **Saito M, Marumo K.** Bone quality in diabetes. *Front. Endocrinol. (Lausanne).* 2013;4(JUN):1–9.

73. **Nair AK, Gautieri A, Chang S-W, Buehler MJ.** Molecular mechanics of mineralized collagen fibrils in bone. *Nat. Commun.* 2013;4:1724.

74. **Vashishth D, Gibson GJ, Khoury JI, Schaffler MB, Kimura J, Fyhrie DP.** Influence of nonenzymatic glycation on biomechanical properties of cortical bone. *Bone* 2001;28(2):195–201.

75. **Tang SY, Vashishth D.** The relative contributions of non-enzymatic glycation and cortical porosity on the fracture toughness of aging bone. *J. Biomech.* 2011;44(2):330–336.

76. **Wongdee K, Charoenphandhu N.** Update on type 2 diabetes-related osteoporosis. *World J. Diabetes* 2015;6(5):673–8.

77. **Petit MA, Paudel ML, Taylor BC, Hughes JM, Strotmeyer ES, Schwartz A V., Cauley JA, Zmuda JM, Hoffman AR, Ensrud KE.** Bone mass and strength in older men with type 2 diabetes: The osteoporotic fractures in men study. *J. Bone Miner. Res.* 2010;25(2):285–291.

78. **Burghardt AJ, Issever AS, Schwartz A V., Davis KA, Masharani U, Majumdar S, Link TM.** High-resolution peripheral quantitative computed tomographic imaging of cortical and trabecular bone microarchitecture in patients with type 2 diabetes mellitus. *J. Clin. Endocrinol. Metab.* 2010;95(11):5045–5055.

79. **Nilsson AG, Sundh D, Johansson L, Nilsson M, Mellström D, Rudäng R, Zoulakis M, Wallander M, Darelid A, Lorentzon M.** Type 2 Diabetes Mellitus Is Associated With Better Bone Microarchitecture But Lower Bone Material Strength and Poorer Physical Function in Elderly Women: A Population-Based Study. *J. Bone Miner. Res.*

2017;32(5):1062–1071.

80. **Furst JR, Bandeira LC, Fan WW, Agarwal S, Nishiyama KK, Mcmahon DJ, Dworakowski E, Jiang H, Silverberg SJ, Rubin MR.** Advanced glycation endproducts and bone material strength in type 2 diabetes. *J. Clin. Endocrinol. Metab.* 2016;101(6):2502–2510.

81. **Farr JN, Drake MT, Amin S, Melton LJ, McCready LK, Khosla S.** In vivo assessment of bone quality in postmenopausal women with type 2 diabetes. *J. Bone Miner. Res.* 2014;29(4):787–795.

82. **Leslie WD, Aubry-Rozier B, Lamy O, Hans D.** TBS (trabecular bone score) and diabetes-related fracture risk. *J. Clin. Endocrinol. Metab.* 2013;98(2):602–609.

83. **Farr JN, Drake MT, Amin S, Melton LJ, McCready LK, Khosla S.** In vivo assessment of bone quality in postmenopausal women with type 2 diabetes. *J. Bone Miner. Res.* 2014;29(4):787–95.

84. **Leanza G, Maddaloni E, Pitocco D, Conte C, Palermo A, Maurizi AR, Pantano AL, Suraci C, Altomare M, Strollo R, Manfrini S, Pozzilli P, Schwartz A V., Napoli N.** Risk factors for fragility fractures in type 1 diabetes. *Bone* 2019;125(December 2018):194–199.

Figure 1 (A) Determinants of bone quality, **(B)** The extraction of cylindrical trabecular bone cores, each 5 mm in diameter and 8-9 mm in length, from femoral heads along the direction of the principal trabeculae using the drilling machine attached with diamond core bit, **(C)** Characterization techniques used to determine the human trabecular bone quality for diabetes patients; SB: subchondral bone

Figure 2 (A) Calculated typical stress-strain plot of compression test for diabetic and non-diabetic groups, **(B)** Amide I and Amide II bond positions in principal structural unit of collagen in human trabecular bone

Figure 3 Representative 3D reconstructed μCT image: **(A)** represents the non-diabetic group and **(B)** represents the diabetic group. The color map in **(C)** and **(D)** represents the variation in trabecular thickness for non-diabetic and diabetic group respectively, **(E-L)** Elastic modulus, yield stress, ultimate stress, yield strain, ultimate strain, post-yield strain, post-yield energy, and toughness respectively, for diabetic and non-diabetic group

Figure 4 (A-B) Reduced modulus (Er) and hardness respectively obtained from nanoindentation, showing smaller value in the diabetic (T2D) group, **(C)** Representative TGA curves with their respective first derivatives for diabetic and non-diabetic femur trabecular bone heated to 1000 °C. The TGA first derivative plots represent the more accurate temperature values associated with the percentage of mass lost, here it can be observed that superficial water completely evaporates before 200 °C, and between 200-600 °C the degradation and combustion of the bone matrix occurs, **(D)** Mineral-to-matrix ratio graph, showing a smaller ratio in the diabetic group *p<0.05

Figure 5 (A) Representative XRD pattern ($20° < 2\theta < 45°$) of human femoral trabecular bone. The peak at 26° and 40° is used to determine the average crystal length and width in the c-axis direction and ab-plane respectively according to Scherrer equation $B(2\theta) = \lambda/L\cos\theta$. Where, B is the mean crystal size, λ is the x-ray wavelength (1.5406 A˚), L is the peak width at half maximum and θ is the Bragg angle where the peak is located, **(B-C)** Mean crystal size graph, showing the insignificant difference in average crystal length but wider width of mean crystal in the diabetic group

Figure 6 (A) Representative FTIR spectra with the appropriate label of various bands to analyze the diabetic and non-diabetic femoral trabecular bone, **(B)** represents peak fitting of Amide I band, collagen properties were obtained by peak fitting of Amide I band with

subbands (Gaussian curves) at 1610, 1630, 1645, 1660, 1678 and 1692 cm^{-1}, **(C)** represents schematically the enzymatic (E-xL) and non-enzymatic crosslink (NE-xL) formation in bone collagen, **(D-F)** measures of mineral properties, showing all mineral parameters could not reach to the level of significance, **(G)** represents non-enzymatic cross-link ratio [NE-xLR, (the area ratio of the 1678/1692 cm^{-1} subbands within the Amide I peak, total cross-linking AGEs)], **(H)** represents enzymatic cross-link ratio [E-xLR, the area ratio of the 1660/1678 cm^{-1} subbands within the Amide I peak], **(I)** represents collagen maturity (area ratio of the 1660/1692 cm^{-1} subbands within the Amide I peak), **(J)** showing lower mineral:matrix ratio in the diabetic group

Abbreviations- AI: Amide I, AII: Amide II, E-xLR: enzymatic cross-link ratio, NE-xLR: non-enzymatic cross-link ratio, AGEs: advanced glycation end products

Figure 7 (A) The graph is showing that the fAGEs content is higher in the diabetic group. **(B-C):** Mechanical properties versus a measure of glycation (fAGE and NE-xLR). Graphical data for several mechanical parameters versus total fluorescent AGEs **(B-C)** and NE-xLR **(D)** are shown.

Figure 8 The relationships between bone volume fraction and **A)** modulus, **B)** yield stress, **C)** ultimate stress, **D)** post-yield energy and **E)** toughness between diabetic and non-diabetics are shown. Data are presented along with best-fit lines (solid lines).

Table 1 Baseline demographic, radiographic and biochemical parameters of diabetic and non-diabetic groups

Table 2 Findings on Structural and Compositional determinants of Bone quality

Table 3 Correlation analysis of selected significant variables of diabetic group which has at least one or more significant relationship with at least one other variable

Table 4 Correlation analysis of selected significant variables of non-diabetic group which has at least one or more significant relationship with at least one other variable

Table 1 Baseline demographic, radiographic and biochemical parameters of diabetic and non-diabetic groups

Parameters	Non-diabetic group (n=40)	Diabetic group (n=30)	p value
Gender (females) n, %	25, 62.5	19, 63.3	0.198
Age (years)	69.8 ± 10.2	69.7 ± 10.0	0.961
Biochemical			
Pre-operative HbA1c (%)	5.4 ± 0.4	7.9 ± 1.8	**< 0.001**
Diabetes duration (years)	Na	7.5 ± 2.8	na
Serum calcium (mg/dl)	8.4 ± 0.6	8.5 ± 0.6	0.306
Serum phosphorus (mg/dl)	3.4 ± 0.7	3.4 ± 0.6	0.658
PTH (pg/ml)	39.3 ± 21.0	41.4 ± 38.4	0.791
25-hydroxy Vitamin D (ng/ml)	22.3 ± 8.6	22.5 ± 8.5	0.932
ALP (IU/L)	134.2 ± 75.8	131.2 ± 36.9	0.875
Imaging			
FN aBMD (gm/cm^2)	0.600 ± 0.091	0.578 ± 0.106	0.329
FN T score	-2.6 ± 0.87	-2.5 ± 0.78	0.696
Medications			
Metformin use (n, %)	0	15, 50	
Metformin + Sulfonylurea use (n, %)	0	12, 40	
Metformin + Sulfonylurea + Insulin use (n, %)	0	3, 10	
Anti-osteoporotic treatment[1] (n, %)	2, 5	1, 3.3	

All data are expressed as mean ± SD, na: not applicable; HbA1c: glycosylated hemoglobin A1c; ALP: alkaline phosphatase; FN: Femoral neck; aBMD: areal bone mineral density

[1]bisphosphonate (alendronate)

Table 2 Findings on Structural and Compositional determinants of Bone quality

Characterization techniques		Parameters studied	Study groups		
			Non-Diabetic	Diabetic	p value
Structural Parameter (Micro- CT)		Bone volume fraction (BV/TV) (%)	21.6 ± 5.50	18.53 ± 5.37	**0.031***
		Trabecular thickness (Tb.Th, mm)	0.167 ± 0.029	0.149 ± 0.026	**0.019 ***
		Trabecular separation (Tb.Sp, mm)	0.603 ± 0.149	0.677 ± 0.166	0.095
		Trabecular number (Tb.N, 1/mm)	1.25 ± 0.176	1.15 ± 0.136	**0.033 ***
		Structure model index (SMI)	1.92 ± 0.12	2.39 ± 0.19	**0.037***
		Degree of anisotropy (DA)	0.612 ± 0.102	0.579±0.198	0.475
Composition (TGA)		Water (weight %)	14.8 ± 9.4	11.6 ± 6.2	0.335
		Organic (weight %)	43.4 ± 9.5	50.8 ± 10.1	0.087
		Mineral (dry weight %)	49.3 ± 7.5	40.9 ± 10.7	**0.038***
		Carbonate (weight %)	1.67 ± 0.3	1.67 ± 0.4	0.988
Macro molecular vibrations (FTIR)	Protein structure	Amide I position (cm^{-1})	1643.8 ± 6.3	1647.3 ± 4.4	**0.02***
		Amide II position (cm^{-1})	1543.1 ± 6.1	1547.8 ± 7.02	**0.009****
	Protein content	Amide I band area/1450 band area	6.97 ± 3.87	3.67 ± 2.08	**<0.001*****
		Amide II band area/1450 band area	2.56 ± 1.47	1.22 ± 0.91	**<0.001*****

* p<0.05, ** p<0.01 and ***p<0.001 respectively compared to non-diabetic group, data is expressed as mean ± SD

Table 3 Correlation analysis of selected significant variables of diabetic group which has atleast one or more significant relationship with at least one other variable

Diabetic group	Modulus	Yield strength	Ultimate strength	Yield strain	Ultimate strain	Yield energy	PY-energy	PY-strain	Toughness	BVTV	HbA1c	fAGE	NE-xLR	E-xLR	M:M FTIR	Tb.Th
Modulus	1	**.710****	**.729****	-0.134	0.019	**.548***	**.485***	0.125	**.620****	**.674****	0.048	-0.122	0.187	0.376	0.158	0.41
Yield strength	.710**	1	**.950****	0.306	0.247	**.924****	0.197	0.023	**.499***	**.655****	0.314	0.141	0.306	0.098	0.333	**.633****
Ultimate strength	.729**	.950**	1	0.239	0.299	**.842****	0.368	0.14	**.623****	**.749****	0.253	-0.292	0.294	0.133	0.37	**.670****
Yield strain	-0.134	0.306	0.239	1	**.558****	**.631****	-0.196	-0.172	0.085	0.117	0.111	0.031	0.017	-0.069	0.331	0.092
Ultimate strain	0.019	0.247	0.299	.558**	1	0.395	0.144	**.722****	0.282	0.084	-0.119	0.025	-0.378	-0.082	0.233	0.155
Yield energy	.548*	.924**	.842**	.631**	0.395	1	0.154	-0.057	**.533***	**.560****	0.181	-0.032	0.207	0.032	0.459	**.493***
PY-energy	.485*	0.197	0.368	-0.196	0.144	0.154	1	0.306	**.919****	**.617****	**-.402***	**-.489***	0.042	0.156	0.273	**.484***
PY-strain	0.125	0.023	0.14	-0.172	.722**	-0.057	0.306	1	0.255	0.003	-0.238	0.028	**-.433***	-0.031	-0.033	0.108
Toughness	.620**	.499*	.623**	0.085	0.282	.533*	.919**	0.255	1	**.747****	-0.331	**-.441***	0.094	0.157	0.38	**.613****
BVTV	.674**	.655**	.749**	0.117	0.084	.560**	.617**	0.003	.747**	1	-0.159	**-.488***	0.051	**.526***	0.341	**.804****
HbA1c	0.048	0.314	0.253	0.111	-0.119	0.181	-.402*	-0.238	-0.331	-0.159	1	**.635****	**.561****	-0.307	0.007	-0.269
fAGE	-0.122	0.141	-0.292	0.031	0.025	-0.032	-.489*	0.028	-.441*	-.488*	.635**	1	**.367***	-0.354	**-.487***	**-.454***
NE-xLR	0.187	0.306	0.294	0.017	-0.378	0.207	0.042	-.433*	0.094	0.051	.561**	**.367***	1	-0.37	0.112	-0.001

E-xLR	0.376	0.098	0.133	-0.069	-0.082	0.032	0.156	-0.031	0.157	.526*	-0.307	-0.354	-0.37	1	-0.105	0.145
M:M FTIR	0.158	0.333	0.37	0.331	0.233	0.459	0.273	-0.033	0.38	0.341	0.007	**-.487***	0.112	-0.105	1	0.361
Tb.Th	0.41	.633**	.670**	0.092	0.155	.493*	.484*	0.108	.613**	.804**	-0.269	**-.454***	-0.001	0.145	0.361	1
** Correlation is significant at the 0.01 level (2-tailed) * Correlation is significant at the 0.05 level (2-tailed) PY: post-yield																

Table 4 Correlation analysis of selected significant variables of non-diabetic group which has atleast one or more significant relationship with at least one other variable

Non-diabetic group	Modulus	Yield strength	Ultimate strength	Yield strain	Ultimate strain	Yield energy	PY-energy	PY-strain	Toughness	BVTV	HbA1c	fAGE	NE-xLR	E-xLR	M:M FTIR	Tb.Th
Modulus	1	**.791****	**.767****	0.122	0.164	0.292	**.545****	-0.058	**.477****	**.701****	**-.332***	-0.184	-0.028	0.253	0.261	**.341***
Yield strength	.791**	1	**.974****	0.029	0.077	0.258	**.603****	-0.015	**.569****	**.746****	-0.274	-0.162	-0.033	0.076	0.197	**.441****
Ultimate strength	.767**	.974**	1	0.022	0.069	0.247	**.601****	-0.017	**.576****	**.698****	-0.291	-0.143	-0.035	0.069	0.224	**.431****
Yield strain	0.122	0.029	0.022	1	**.973****	**.972****	**.545****	-0.03	-0.02	0.029	0.039	-0.231	-0.094	**.405***	-0.035	-0.054
Ultimate strain	0.164	0.077	0.069	.973**	1	**.958****	**.607****	0.087	0.079	0.078	-0.044	-0.283	-0.143	**.419***	-0.037	-0.039
Yield energy	0.292	0.258	0.247	.972**	.958**	1	**.675****	-0.042	0.124	0.192	-0.05	-0.272	-0.072	**.389***	0.008	0.067
PY-energy	.545**	.603**	.601**	.545**	.607**	.675**	1	0.055	**.815****	**.405***	-0.243	-.328*	-0.02	0.158	0.085	0.186
PY-strain	-0.058	-0.015	-0.017	-0.03	0.087	-0.042	0.055	1	0.113	-0.121	0.105	-0.137	-0.223	0.097	-0.008	-0.1
Toughness	.477**	.569**	.576**	-0.02	0.079	0.124	.815**	0.113	1	**.370***	-0.283	-0.232	0.029	-0.147	0.102	0.211
BVTV	.701**	.746**	.698**	0.029	0.078	0.192	.405*	-0.121	.370*	1	-0.266	0.009	-0.108	0.103	0.09	**.566****
HbA1c	-.332*	-0.274	-0.291	0.039	-0.044	-0.05	-0.243	0.105	-0.283	-0.266	1	**.296***	**.396****	**-.353***	-0.057	-0.125
fAGE	-0.184	-0.162	-0.143	-0.231	-0.283	-0.272	-.328*	-0.137	-0.232	0.009	.296*	1	0.019	-0.111	-0.205	**.315***
NE-xLR	-0.028	-0.033	-0.035	-0.094	-0.143	-0.072	-0.02	-0.223	0.029	-0.10	.396**	0.019	1	**-.430**	-0.107	-0.01

										8				**		4
E-xLR	0.253	0.076	0.069	.405*	.419*	.389*	0.158	0.097	-0.147	0.103	-.353*	-0.111	-.430**	1	0.128	0.219
M:M FTIR	0.261	0.197	0.224	-0.035	-0.037	0.008	0.085	-0.008	0.102	0.09	-0.057	-0.205	-0.107	0.128	1	-0.185
Tb.Th	.341*	.441**	.431**	-0.054	-0.039	0.067	0.186	-0.1	0.211	.566**	-0.125	.315*	-0.014	0.219	-0.185	1

** Correlation is significant at the 0.01 level (2-tailed)
* Correlation is significant at the 0.05 level (2-tailed),
PY: post-yield

Figure 1

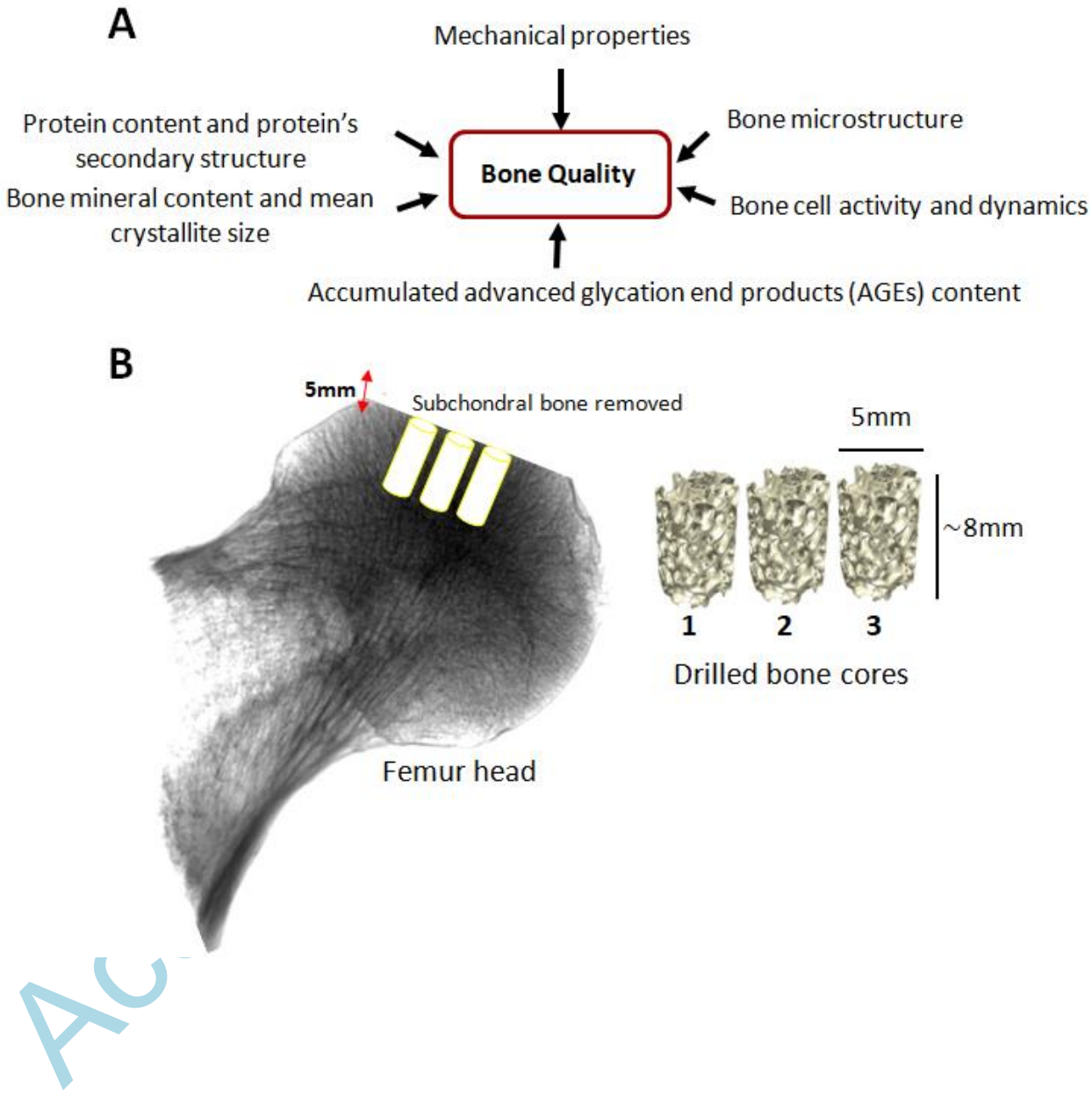

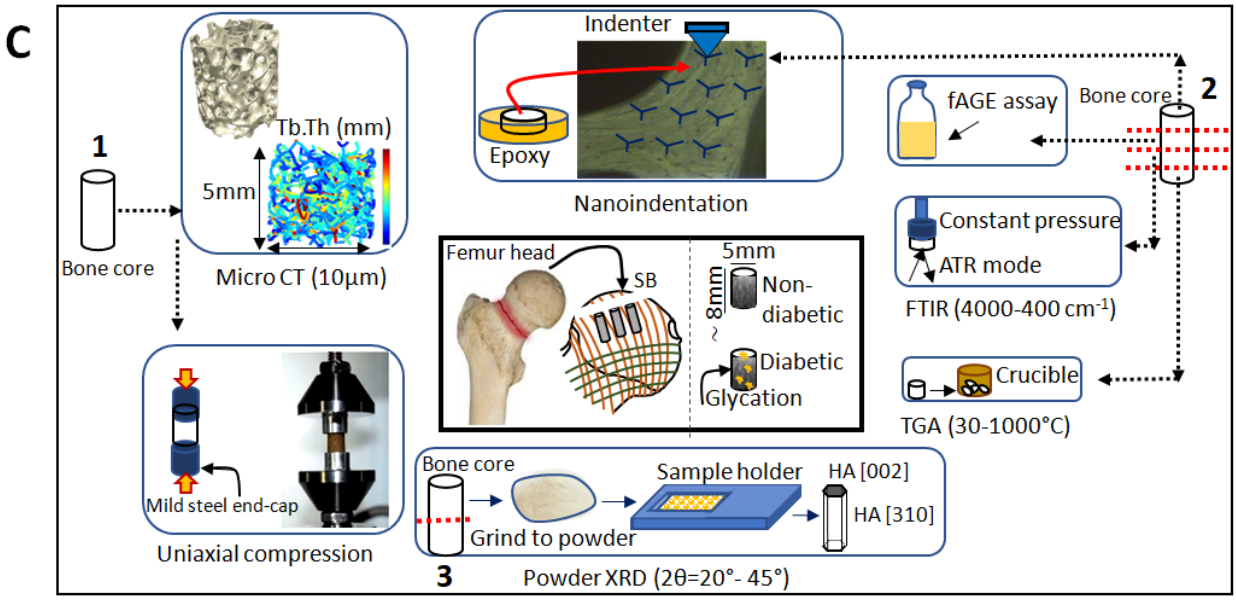

Figure 2

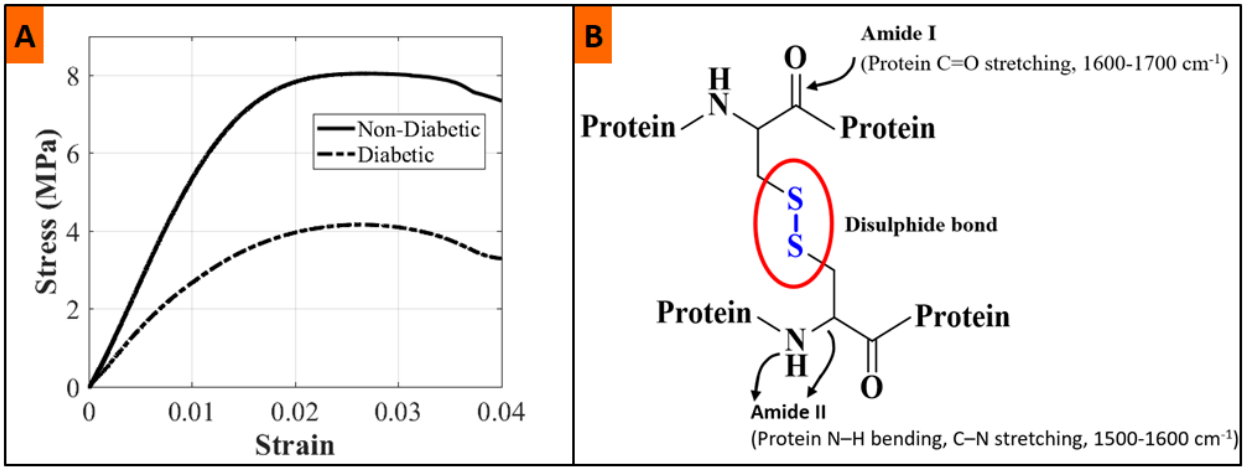

Figure 3

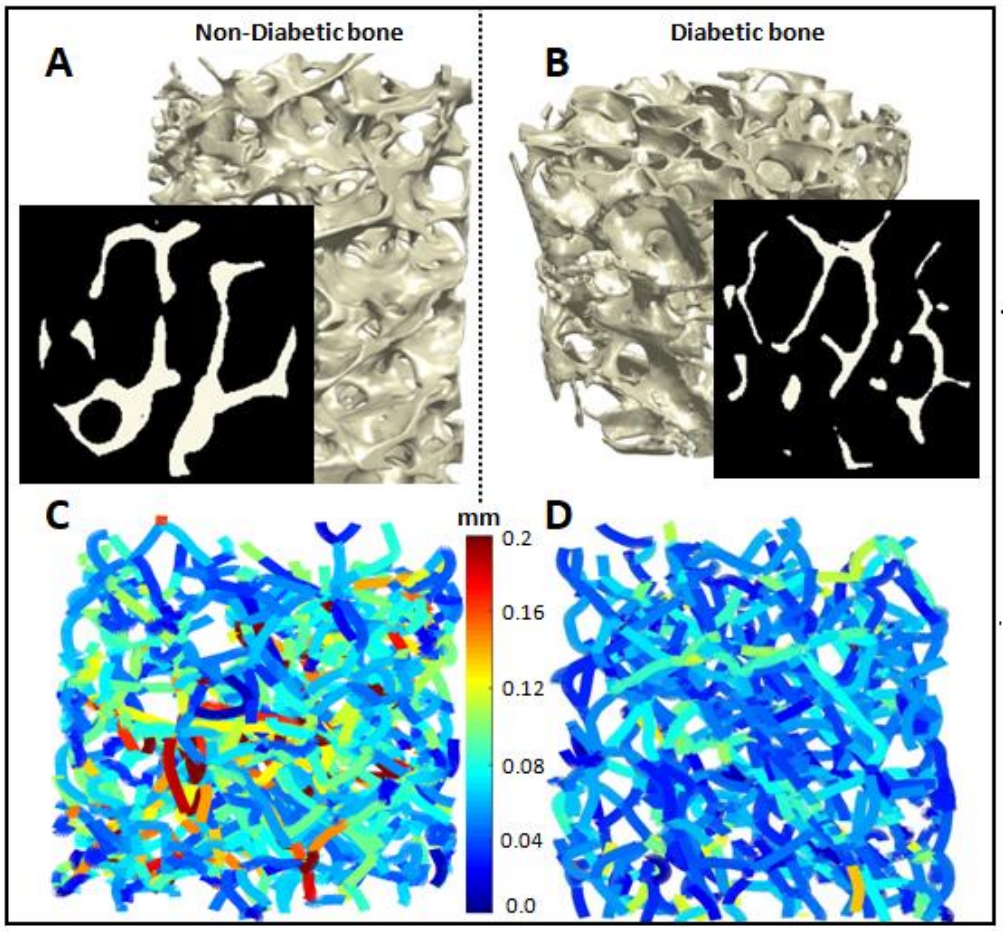

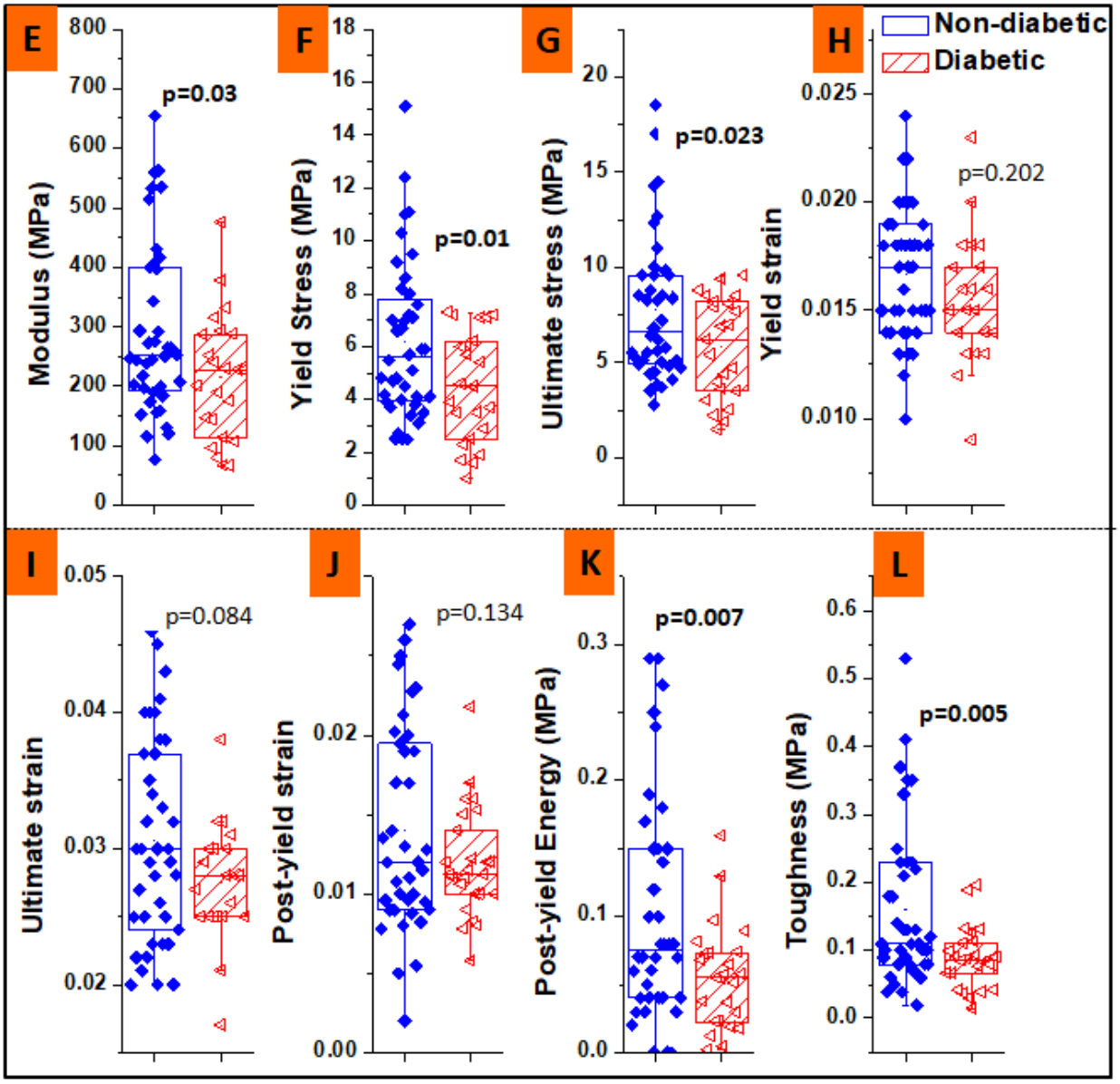

Figure 4

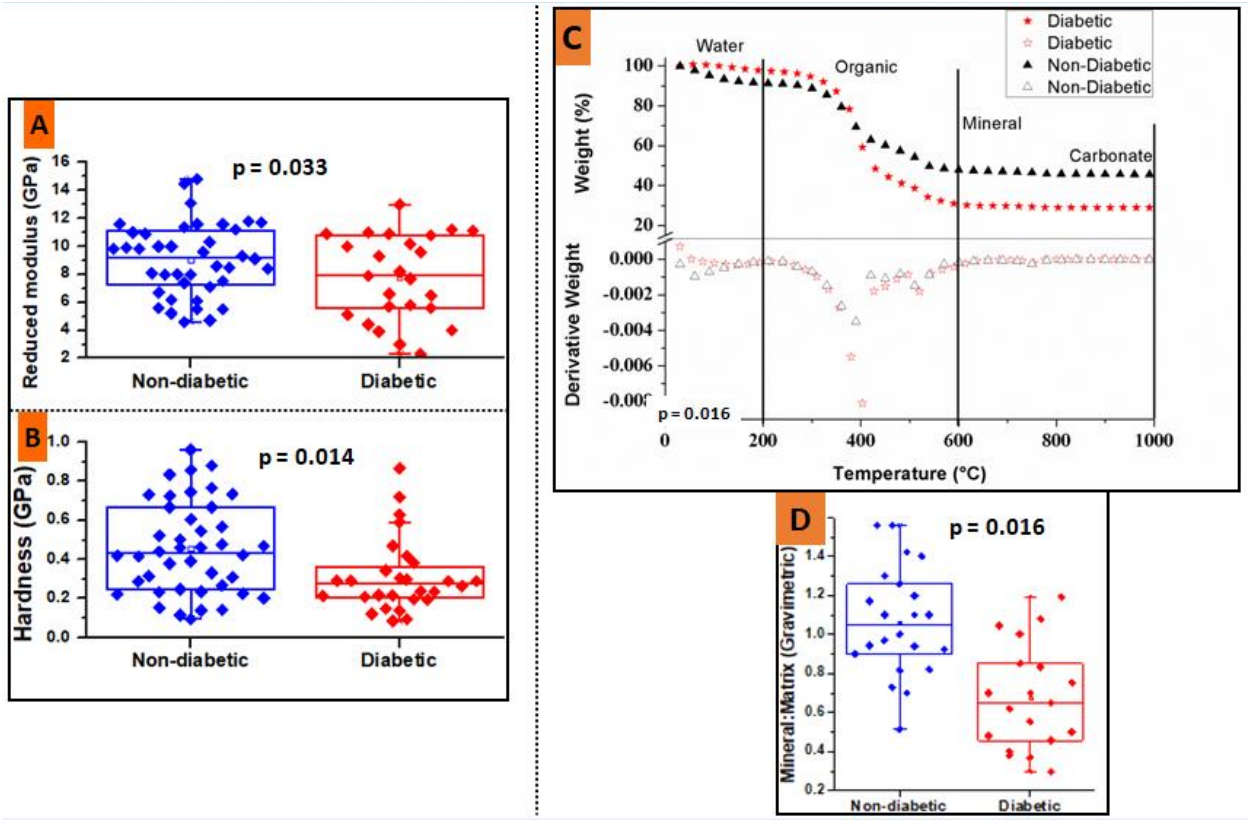

Figure 5

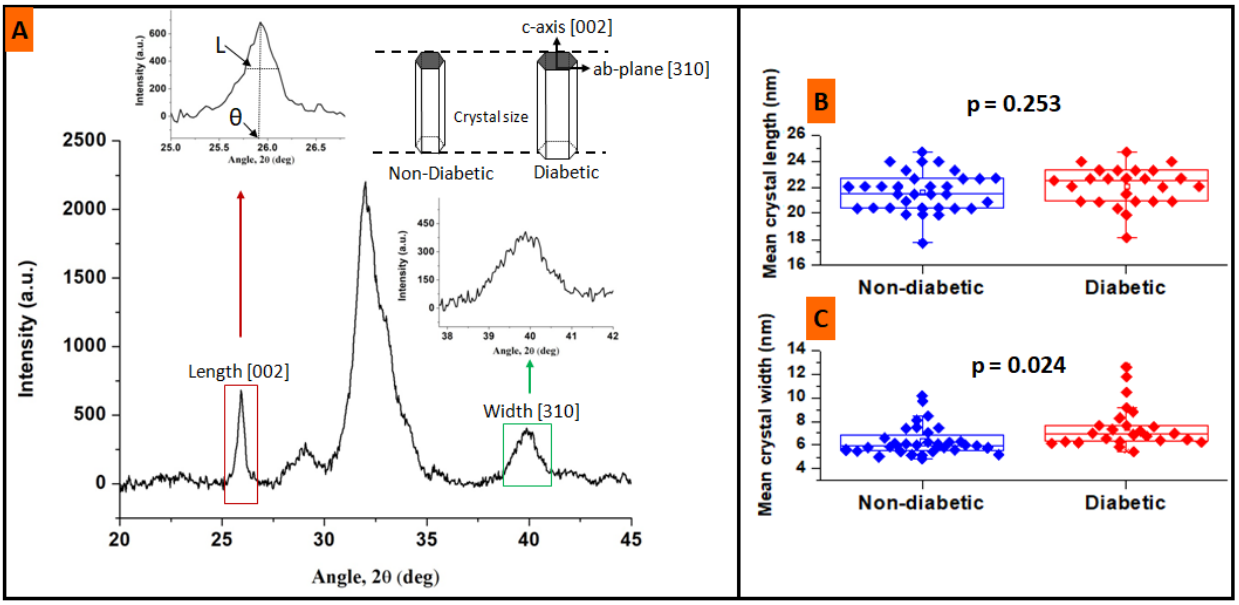

Figure 6

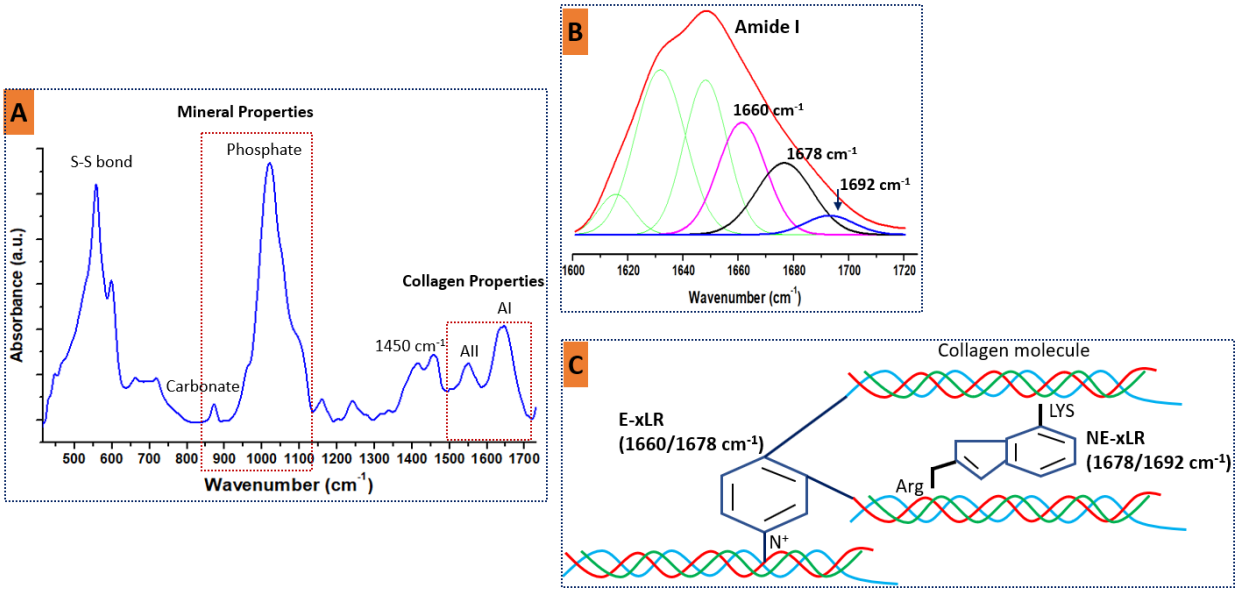

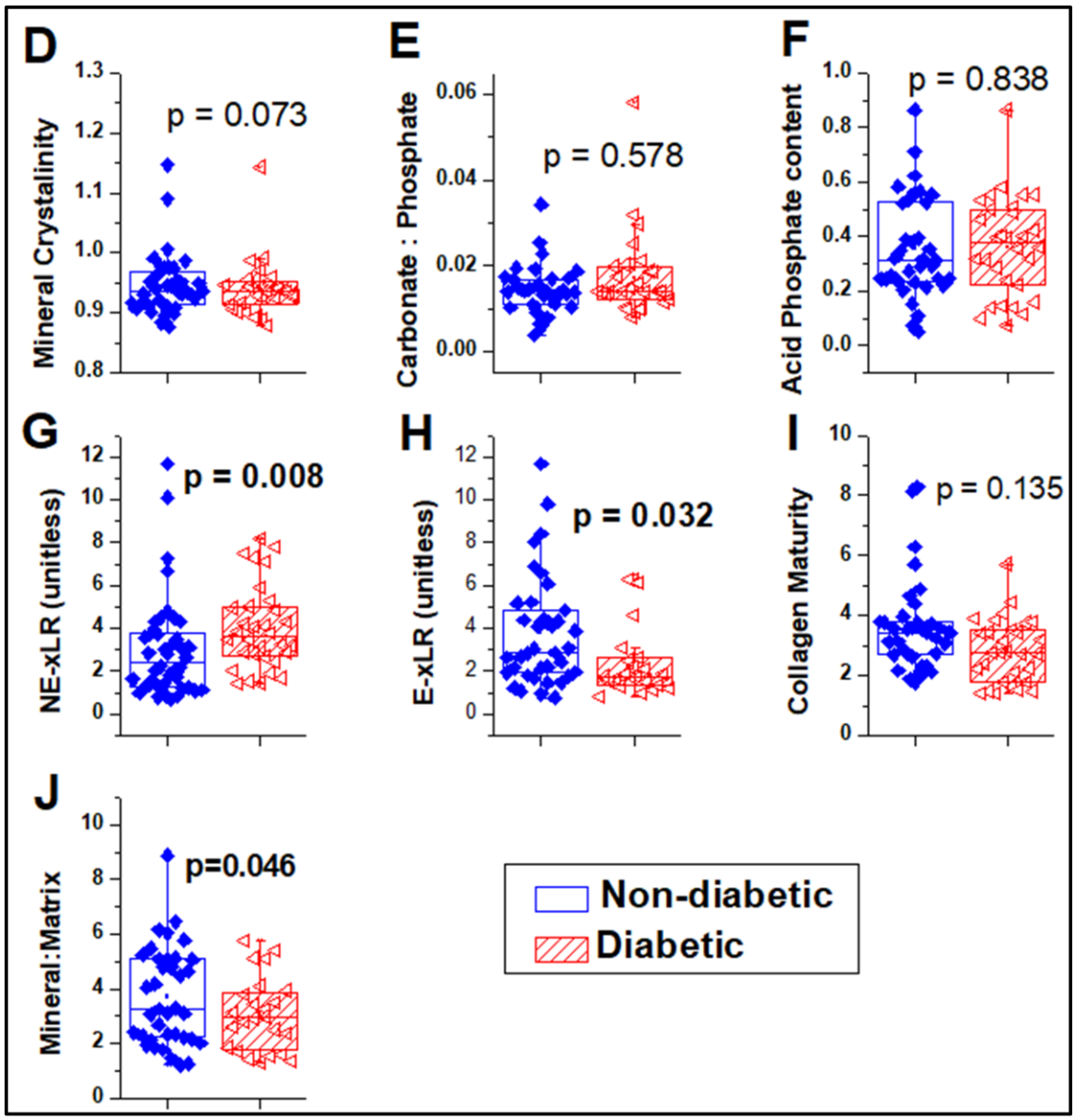

Figure 7

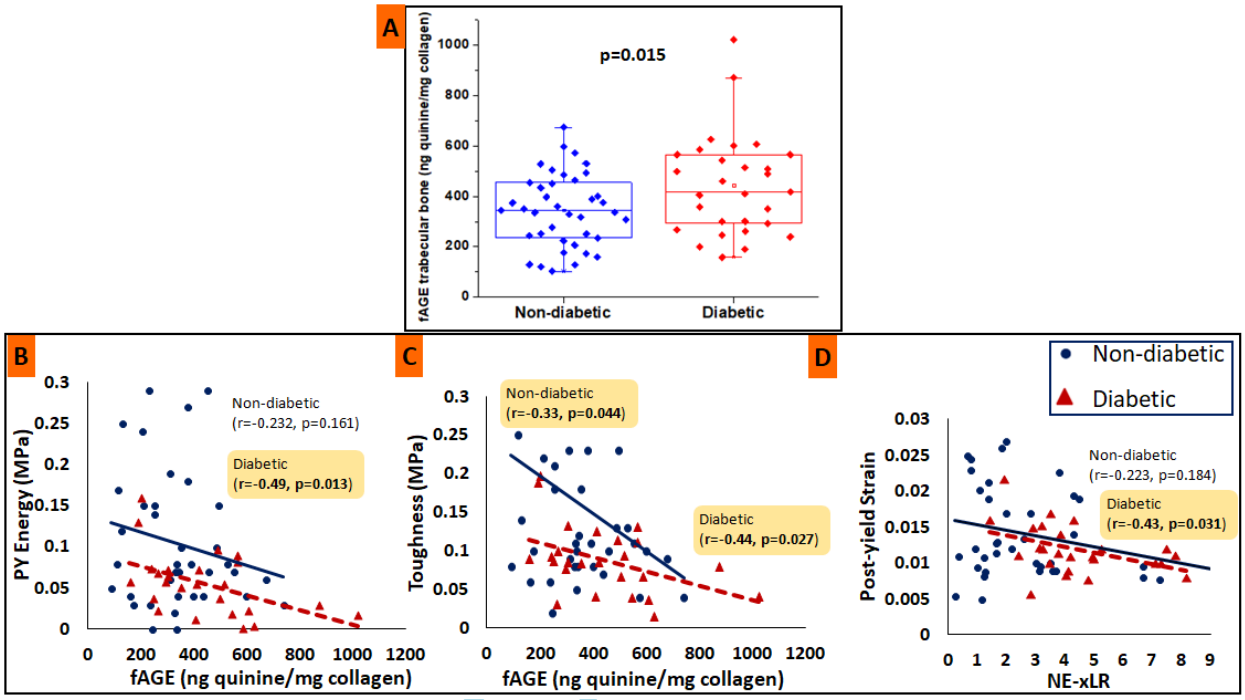

Figure 8